

NANO EXPRESS

Open Access

Improved ground-state modulation characteristics in 1.3 μm InAs/GaAs quantum dot lasers by rapid thermal annealing

Hanxue Zhao^{1*}, Soon Fatt Yoon^{1†}, Chun Yong Ngo^{2†} and Rui Wang^{1†}

Abstract

We investigated the ground-state (GS) modulation characteristics of 1.3 μm InAs/GaAs quantum dot (QD) lasers that consist of either as-grown or annealed QDs. The choice of annealing conditions was determined from our recently reported results. With reference to the as-grown QD lasers, one obtains approximately 18% improvement in the modulation bandwidth from the annealed QD lasers. In addition, the modulation efficiency of the annealed QD lasers improves by approximately 45% as compared to the as-grown ones. The observed improvements are due to (1) the removal of defects which act as nonradiative recombination centers in the QD structure and (2) the reduction in the Auger-related recombination processes upon annealing.

Introduction

Quantum dots (QDs) are promising for realizing fast and stable laser sources in fiber optic applications, due to their superior characteristics over conventional quantum well (QW) lasers, such as low threshold current, high internal efficiency, and infinite characteristic temperature [1,2]. However, the high-speed performance of QDs is generally poorer than that of QWs due to several factors: slow inter-level relaxation of the carriers [3], finite density of state (DOS), and closely spaced hole energy levels [4]. Slow carrier relaxation rate, in combination with the limited DOS, will lead to early switching from ground-state (GS) lasing to excited-state (ES) lasing at high temperature or at high drive current. This is undesired since ES lasing reduces GS lasing efficiency due to gain saturation of the GS transition. This, due to state filling effect in discrete quantum levels, degrades the high-speed characteristics [2,5] of the QD lasers. Furthermore, for high-speed modulation, shorter cavity length is favored. Unfortunately, transition from GS to ES lasing occurs earlier in short cavity lasers (≤ 1 mm) due to the increased cavity loss as compared to long cavity lasers [3]. Thus, to improve the high-speed

performance of QD lasers, it is important to delay the onset of ES lasing. It is well-documented that *p*-doping of the QDs can reduce the effect of gain saturation and thus maintain GS lasing up to higher operating temperatures [1], and potentially faster relaxation time [6]. On the other hand, rapid thermal annealing (RTA) might result in intermixing of the QDs with the surrounding matrix and tunable inter-level energy. This may lead to faster inter-level relaxation of the carriers [7], and consequently, suppression of ES lasing and improved high-speed modulation efficiency. However, there exists only a handful of works on the effects of RTA on GS modulation of the annealed *p*-doped QD lasers [8-10].

In this work, we have investigated the effect of RTA on the GS modulation characteristics of 1.3 μm *p*-doped InAs/GaAs QD lasers. Both the modulation bandwidth and efficiency were found to increase significantly upon annealing.

Experimental details

The ten-layer self-assembled *p*-doped InAs/GaAs QD laser structure used in this experiment was grown on GaAs (100) substrate by molecular beam epitaxy (MBE). The structure consists of QD active region sandwiched between two 1.5 μm C- and Si-doped $\text{Al}_{0.35}\text{Ga}_{0.65}\text{As}$ cladding layers. The active layer comprises 2.3 monolayer (ML) of InAs QDs capped by a 5-nm $\text{In}_{0.15}\text{Ga}_{0.85}\text{As}$ layer.

* Correspondence: zhao0097@e.ntu.edu.sg

† Contributed equally

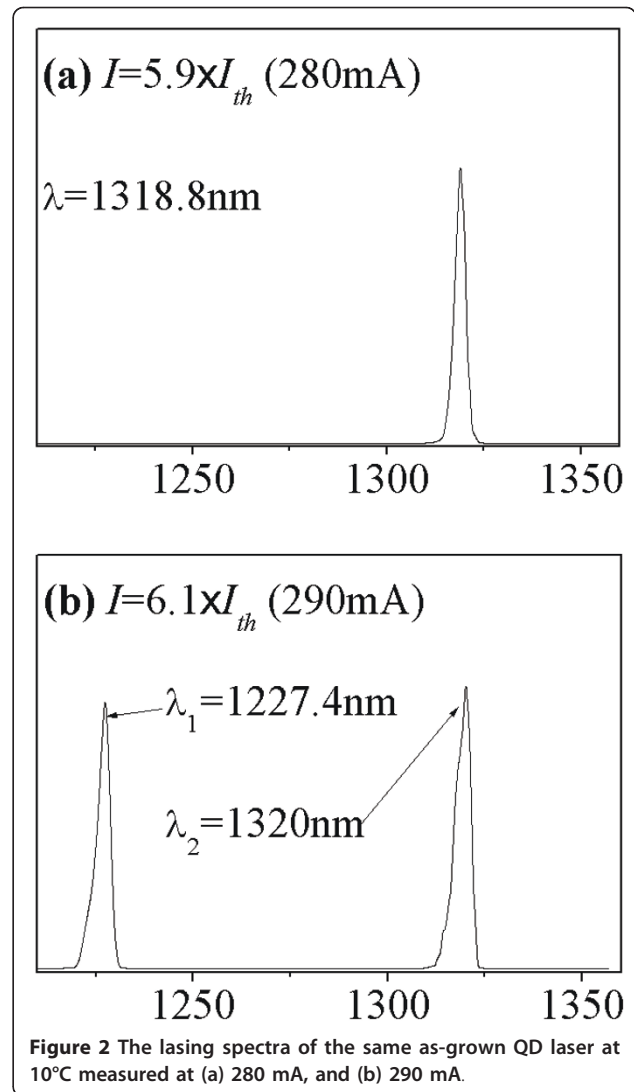
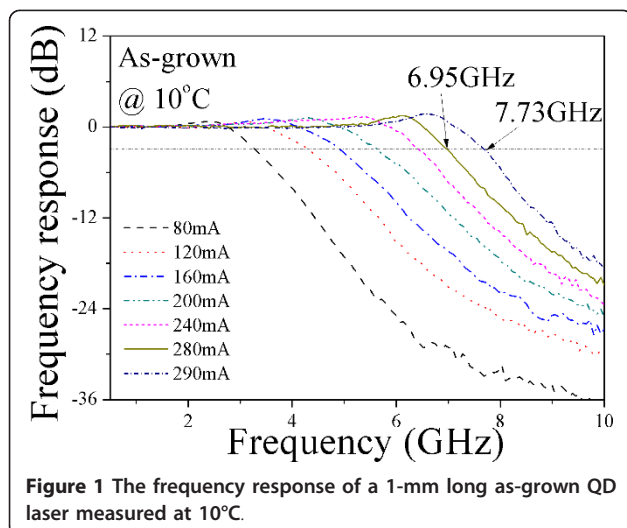
¹School of Electrical and Electronic Engineering, Nanyang Technological University, Singapore 639798, Singapore

Full list of author information is available at the end of the article

A 33-nm GaAs layer is used to separate the two QD layers. P-doping modulation (~16 acceptors per QD) was incorporated into the 10 nm GaAs layer in the middle of each 33 nm-thick spacer between the QD rows [11]. The indium-containing layers were grown at approximately 485°C, while the (Al)GaAs layers were grown at approximately 580°C. The QD samples were capped with 200 nm of SiO₂ deposited by plasma-enhanced chemical vapor deposition (PECVD) before annealing. The annealing process was then performed in N₂ ambient at 600°C for 15 s using a rapid thermal processor. The choice of annealing conditions was determined from our recently reported results [9]. Subsequently, the as-grown and annealed samples were processed into 4-μm-wide narrow ridge waveguide lasers [12]. The high-speed modulation of the as-cleaved QD lasers was performed under continuous-wave (CW) biasing condition using a vector network analyzer (VNA) and a high-speed photoreceiver [13]. The spontaneous emission intensity of the device under different bias currents was obtained with an integrating sphere. A thermoelectric temperature controller controls the device temperature during measurements.

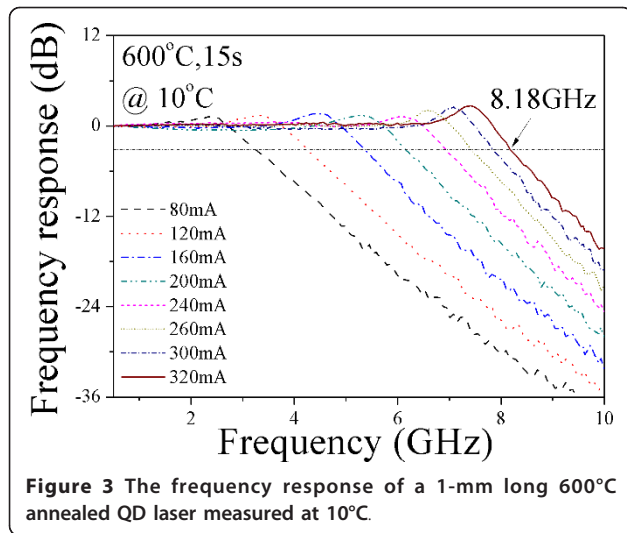
Results and discussion

Figure 1 shows the frequency response of the as-grown device with cavity length of 1 mm, measured at 10°C. The threshold current (I_{th}) of the as-grown device is approximately 51.6 mA. The bandwidth increases gradually with bias currents. The maximum bandwidth obtained is 7.73 GHz. Figure 2 shows the lasing spectra of the same as-grown QD laser at 10°C measured at (a) 280 mA, and (b) 290 mA. Note that the ES lasing threshold ($I_{th,ES}$) of the as-grown device is 284 mA. At the bias current of $5.9 \times I_{th}$ (280 mA), the laser emission wavelength is approximately 1319 nm and corresponds to the GS lasing (refer to Figure 2a). When increasing

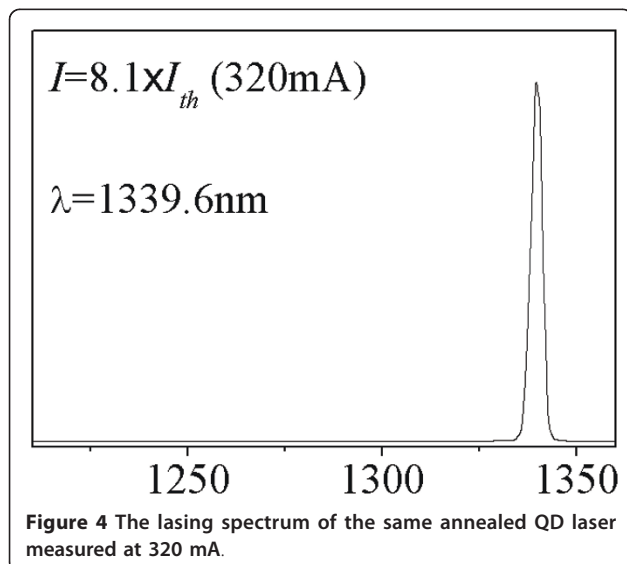


the bias current to $6.1 \times I_{th}$ (290 mA), emission wavelengths of approximately 1227 and 1320 nm exist simultaneously (refer to Figure 2b). The energy separation between the two states is approximately 71 meV. Thus, in the as-grown laser, GS lasing dominates at low bias currents, while ES lasing dominates at higher bias currents. The bandwidth of 7.73 GHz for the as-grown device measured at 290 mA includes the contribution from ES lasing. The bandwidth obtained from purely GS lasing is 6.95 GHz at 280 mA. Slight increase of the bias current by 10 mA causes a significant increase of bandwidth by 0.78 GHz (from 6.95 to 7.73 GHz), which is likely due to the additional photons emitted by the ES lasing. However, the bandwidth contributed by ES lasing is undesired since the wavelength of interest for telecommunication is 1.3 μm.

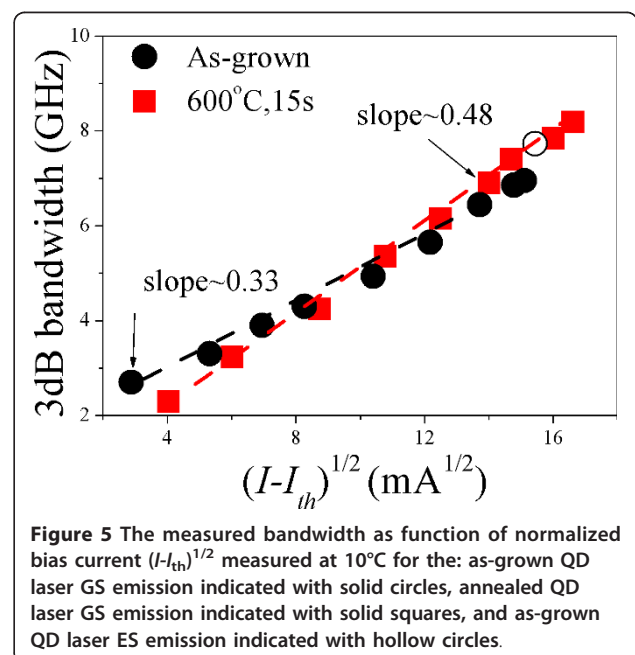
Figure 3 shows the frequency response for the 600°C annealed device with cavity length of 1 mm, at 10°C.



The I_{th} of the 600°C annealed device is approximately 42.6 mA. The lasing spectrum of the 600°C annealed device at $8.1 \times I_{th}$ (320 mA) is shown in Figure 4. Since the bandwidth saturates at current greater than 320 mA, the maximum bandwidth obtained is 8.18 GHz. After annealing, 18% improvement in modulation bandwidth has been achieved. It is worth mentioning that no ES lasing has been observed in the annealed laser for all bias current levels. Therefore, the maximum bandwidth of 8.18 GHz for the 600°C annealed device is purely from GS lasing. Comparing Figure 2a and Figure 4, the difference in the GS wavelength might be due to the carrier induced bandgap shrinkage [14] and the thermal induced emission wavelength shift [15-17]. At a fixed current injection above threshold, a higher I/I_{th} ratio is resultant in the annealed lasers ($8.1 \times I_{th}$) than in the

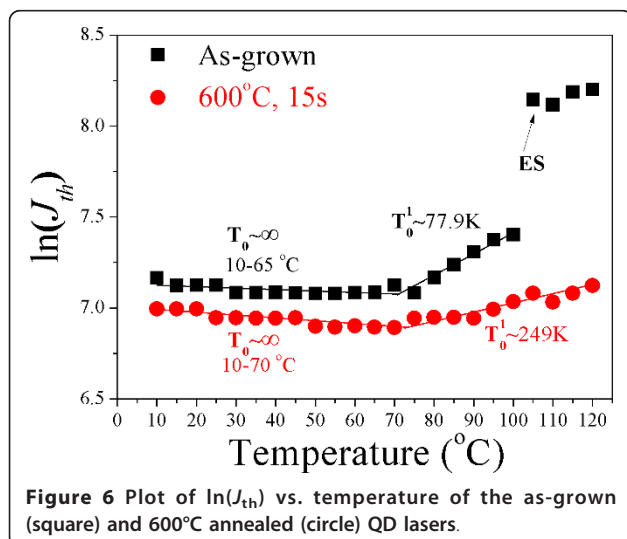


as-grown lasers ($5.9 \times I_{th}$) due to the reduction of threshold current after annealing [13]. The thermal effects may become more dominant in affecting the wavelength due to annealing. The reasons of this wavelength shift are currently under investigation. Figure 5 shows the measured bandwidth as function of normalized bias current $(I-I_{th})^{1/2}$ measured at 10°C for the: as-grown QD laser GS emission indicated with solid circles, annealed QD laser GS emission indicated with solid squares, and as-grown QD laser ES emission indicated with hollow circles. The slope deduced from the bandwidth vs. $(I-I_{th})^{1/2}$ (also known as modulation efficiency, η_{MOD}) is approximately 0.33 GHz/mA^{1/2} for the as-grown device at low bias. Note that there is a sudden increase of the η_{MOD} when ES lasing starts to dominate. GS lasing dominates in the 600°C annealed device throughout the measured bias current range, while ES lasing has been completely suppressed, even at higher bias currents. The η_{MOD} for the 600°C annealed device is approximately 0.48 GHz/mA^{1/2}. Note that the η_{MOD} has been increased by approximately 45% after the 600°C RTA process. Shi et al. [3] have shown that fast inter-level relaxation is favorable for the GS lasing, and leads to higher QD GS capture efficiency. When the inter-level relaxation becomes slower, carriers captured into the ES cannot relax to the GS immediately and continues to occupy the ES. The ES lasing will occur when the population inversion for the transition between the ES electrons and the GS holes is satisfied. Higher η_{MOD} in the 600°C annealed laser indicates lower wetting layer carrier occupation probability and higher GS capture



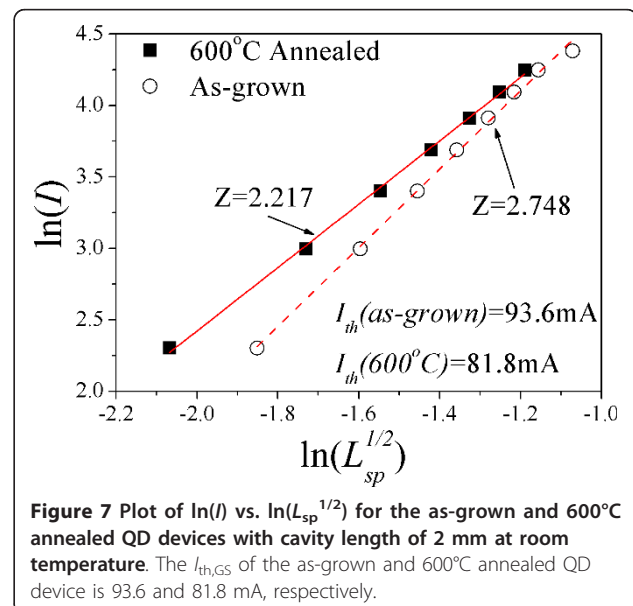
efficiency, which may be due to faster inter-level relaxation induced by RTA [9].

Figure 6 shows the logarithmic values of threshold current densities ($\ln(J_{th})$) of as-grown and 600°C annealed devices measured as function of temperature. The as-grown and 600°C annealed lasers exhibit infinite T_0 at temperature range of 10-65 and 10-70°C, respectively. The infinite T_0 could be explained by the increase in Auger recombination and improved carrier thermalization with increasing temperature. The former will increase the threshold current, while the latter decreases the threshold current by increasing the efficiency of the radiative recombination due to thermal escape of carriers from the dots and transfer into deeper levels (larger dots) [1]. Due to *p*-type modulation doping in the QDs, the electrostatic attraction of the excess holes increases the effective barrier for electron escape, thus limits the electron thermalization till higher temperature as compared to the intrinsic device and results in a larger T_0 [18]. The as-grown laser exhibits $T_0^1 \sim 77.9$ K from 70 to 100°C. ES-dominated lasing starts at 105°C in the as-grown laser. However, in the annealed laser, GS lasing dominates throughout the measured temperature range, up to 120°C. The annealed laser exhibits $T_0^1 \sim 249$ K from 75 to 120°C. As shown in Figure 6, as compared to the as-grown lasers, the threshold current has been reduced and T_0^1 has been improved for the annealed QDs up to 120°C. These are possibly due to the reduction in Auger recombination in the annealed QDs since Auger recombination increases the threshold current. In agreement with the work of Shchekin et al. [19], the modulation response of QD laser is closely related to the threshold characteristics. Although QDs have been predicted to be modulated at very high frequencies theoretically, it has been shown by Deppe et al. [4] that the current densities required to reach these values should be



considered. The low threshold current density of the annealed QD laser suggests that this device can be driven far above threshold and reaches higher speed. It has been pointed out by Marko et al. that Auger recombination is an important loss process in 1.3 μm QD lasers around room temperature [18]. *p*-Doping of the QDs enhances the gain, but it also increases the threshold current, possibly due to increased Auger recombination [20]. The improved T_0 , together with the reduced threshold current density in the annealed lasers, implies that the severe non-radiative Auger recombination is possibly reduced as a consequence of thermal annealing by reducing the defect densities. And this potential results in improved carrier relaxation, thus improved high-speed modulation characteristics.

Figure 7 shows the plot of $\ln(I)$ vs. $\ln(L_{sp}^{1/2})$, where I is the injection current and L_{sp} is the total spontaneous emission intensity. The gradient obtained is known as the Z value. The total spontaneous emission intensity is measured by modulating the device in the unamplified region, where $I < I_{th}$. Over this limited range of I , we employed a general relationship between I and L_{sp} [21]: $\ln(I) \propto Z \ln(L_{sp}^{1/2})$, where $1 \leq Z \leq 3$, depending on the relative importance of nonradiative monomolecular recombination process due to defects or impurities ($Z = 1$), bimolecular radiative recombination process ($Z = 2$) or nonradiative Auger recombination process ($Z = 3$). Generally, $2 \leq Z \leq 3$ applies in InAs/GaAs QDs, especially in *p*-doped QDs, due to the enhanced nonradiative Auger recombination [22]. As shown in Figure 7, Z reduces from 2.748 for the as-grown device to 2.217 for the annealed device. This suggests that the radiative recombination becomes more dominant than the Auger-related recombination processes



resulting from annealing [21]. It is thus reasonable to say that the radiative recombination has been enhanced after 600°C RTA. The suppression of nonradiative Auger recombination may also result in smaller carrier lifetime, thus improved high-speed modulation performances, which agrees well with our experimental results on the improved small signal modulation performances in annealed lasers (as shown in Figures 1, 3, 5). Furthermore, our experimental results also demonstrate improved quantum efficiency and reduced optical loss in the 600°C annealed lasers, which have been submitted elsewhere [9].

Conclusions

In summary, we have investigated the GS modulation characteristics of 1.3 μm InAs/GaAs QD lasers that consist of either as-grown or annealed QDs. Compared to the as-grown QD lasers, the annealed ones exhibit approximately 18% improvement in the modulation bandwidth and approximately 45% in the modulation efficiency. The observed improvements are due to the reduction in the Auger-related recombination processes and the removal of nonradiative recombination centers in the QDs upon annealing.

Abbreviations

CW: continuous-wave; DOS: density of state; ES: excited-state; GS: ground-state; MBE: molecular beam epitaxy; ML: monolayer; PEVCD: plasma-enhanced chemical vapor deposition; QD: quantum dot; QW: quantum well; RTA: rapid thermal annealing; VNA: vector network analyzer.

Author details

¹School of Electrical and Electronic Engineering, Nanyang Technological University, Singapore 639798, Singapore ²Patterning & Fabrication Capability Group, Institute of Materials Research & Engineering, 3 Research Link, Singapore

Authors' contributions

ZHX: conceived of the study, participated in the device fabrications, carried out the static and small signal characterizations, performed the experimental analyses, and drafted the manuscript, YSF: conceived of the study, and participated in its design and coordination, CYN: performed the Rapid Thermal Annealing, and participated in the design and coordination of the study, WR: conceived of the study, participated in its design and coordination, and participated in the device fabrications. All authors read and approved the final manuscript.

Competing interests

The authors declare that they have no competing interests.

Received: 11 March 2011 Accepted: 16 May 2011

Published: 16 May 2011

References

- Masse NF, Sweeney SJ, Marko IP, Adams AR, Hatori N, Sugawara M: Temperature dependence of the gain in p-doped and intrinsic 1.3 μm InAs/GaAs quantum dot lasers. *Appl Phys Lett* 2006, **89**:191118.
- Markus A, Chen JX, Paranthoen C, Fiore A, Platz C, Gauthier-Lafaye O: Simultaneous two-state lasing in quantum-dot lasers. *Appl Phys Lett* 2003, **82**:1818.
- Shi LW, Chen YH, Xu B, Wang ZC, Wang ZG: Effect of inter-level relaxation and cavity length on double-state lasing performance of quantum dot lasers. *Phys E* 2007, **39**:203.

- Deppe DG, Huang H, Shchekin OB: Modulation characteristics of quantum-dot lasers: The influence of p-type doping and the electronic density of states on obtaining high speed. *IEEE J Quantum Electron* 2002, **38**:1587.
- Liu HY, Childs DT, Badcock TJ, Groom KM, Sellers IR, Hopkinson M, Hogg RA, Robbins DJ, Mowbray DJ, Skolnick MS: High-performance three-layer 1.3-μm InAs-GaAs quantum-dot lasers with very low continuous-wave room-temperature threshold currents. *IEEE Photon Technol Lett* 2005, **17**:1139.
- Tong CZ, Xu DW, Yoon SF: Carrier relaxation and modulation response of 1.3-μm InAsGaAs quantum dot lasers. *J Lightwave Technol* 2009, **27**:5442.
- Malik S, Le Ru EC, Childs D, Murray R: Time-resolved studies of annealed InAs/GaAs self-assembled quantum dots. *Phys Rev B* 2001, **63**:155313.
- Lee HS, Lee JY, Kim TW, Kim MD: Effect of thermal annealing on the microstructural and optical properties of vertically stacked InAs/GaAs quantum dots embedded in modulation-doped heterostructures. *J Appl Phys* 2003, **94**:6354.
- Cao Q, Yoon SF, Tong CZ, Ngo CY, Liu CY, Wang R, Zhao HX: Two-state competition in 1.3-μm multilayer InAs/InGaAs quantum dot lasers. *Appl Phys Lett* 2009, **95**:191101.
- Cao Q, Yoon SF, Liu CY, Tong CZ: Effects of rapid thermal annealing on optical properties of p-doped and undoped InAs/InGaAs dots-in-a-well structures. *J Appl Phys* 2008, **104**:033522.
- Cao Q, Yoon SF, Liu CY, Ngo CY: Narrow ridge waveguide high power single mode 1.3-μm InAs/InGaAs ten-layer quantum dot lasers. *Nanoscale Res Lett* 2007, **2**:303.
- Zhao HX, Yoon S, Tong CZ, Liu CY, Wang R, Cao Q: Thermal effects and small signal modulation of 1.3-μm InAs/GaAs self-assembled Quantum-Dot lasers. *Nanoscale Res Lett* 2010, **6**:37.
- Zhao HX, Yoon SF, Ngo CY, Wang R, Tong CZ, Liu CY, Cao Q: Effects of thermal annealing on the dynamic characteristics of InAs/GaAs quantum dot lasers. *Photon J IEEE* 2010, **2**:630.
- Kim JS, Lee CR, Seol KW, Oh DK: Wavelength shift of InP-based InAs quantum dot lasers above room temperature. *J Nanosci Nanotechnol* 2007, **7**:4443.
- Deubert S, Debusmann R, Reithmaier JP, Forchel A: High-power quantum dot lasers with improved temperature stability of emission wavelength for uncooled pump sources. *Electron Lett* 2005, **41**:1125.
- Reithmaier JP, Forchel A: Recent advances in semiconductor quantum-dot lasers. *C R Phys* 2003, **4**:611.
- Klopf F, Reithmaier JP, Forchel A: Highly efficient GaInAs/(Al)GaAs quantum-dot lasers based on a single active layer versus 980 nm high-power quantum-well lasers. *Appl Phys Lett* 2000, **77**:1419.
- Marko IP, Masse NF, Sweeney SJ, Andreev AD, Adams AR, Hatori N, Sugawara M: Carrier transport and recombination in p-doped and intrinsic 1.3 μm InAs/GaAs quantum-dot lasers. *Appl Phys Lett* 2005, **87**:21114.
- Shchekin OB, Deppe DG: The role of p-type doping and the density of states on the modulation response of quantum dot lasers. *Appl Phys Lett* 2002, **80**:2758.
- Fathpour S, Mi Z, Bhattacharya P, Kovsh AR, Mikhrin SS, Krestnikov IL, Kozhukhov AV, Ledentsov NN: The role of Auger recombination in the temperature-dependent output characteristics T₀ = infinity of p-doped 1.3 μm quantum dot lasers. *Appl Phys Lett* 2004, **85**:5164.
- Tanoto H, Yoon SF, Lew KL, Loke WK, Dohrman C, Fitzgerald EA, Tang LJ: Electroluminescence and structural characteristics of InAs/In_{0.1}Ga_{0.9}As quantum dots grown on graded Si_{1-x}Gex/Si substrate. *Appl Phys Lett* 2009, **95**:141905.
- Jang YD, Badcock TJ, Mowbray DJ, Skolnick MS, Park J, Lee D, Liu HY, Hopkinson M, Hogg RA, Andreev AD: Enhanced nonradiative Auger recombination in p-type modulation doped InAs/GaAs quantum dots. *Appl Phys Lett* 2008, **93**:101903.

doi:10.1186/1556-276X-6-382

Cite this article as: Zhao et al.: Improved ground-state modulation characteristics in 1.3 μm InAs/GaAs quantum dot lasers by rapid thermal annealing. *Nanoscale Research Letters* 2011 **6**:382.